The Jameson Cell

Geoffrey M Evans
Bruce W Atkinson
Graeme J Jameson

12

The Jameson Cell

Geoffrey M. Evans, Bruce W. Atkinson, and Graeme J. Jameson
University of Newcastle, Newcastle, New South Wales, Australia

I. INTRODUCTION

The Jameson cell is a type of flotation column in which the air and the pulp are brought together in a vertical tube. The air and pulp are dispersed into a dense foam of fine bubbles, which creates a favorable environment for particle–bubble collision and subsequent collection of hydrophobic particles (1). The bubbly mixture then discharges into the cell proper, which is essentially a disengagement chamber in which the bubbles carrying the floatable particles separate from the pulp. The disengagement zone behaves in a similar fashion to the froth zone in a conventional flotation column, and as in the column, it is possible to apply clean washwater to the froth to remove unwanted gangue particles.

The main advantages of the Jameson cell relate to the rapid collection of particles in the downcomer, leading to a compact space-efficient device, and to the ability of the cell to operate with self-aspiration, thus obviating the need for compressors or blowers.

Since its introduction at the commercial scale in 1989, the cell has been applied to a variety of ores, and full-sized cells are now operating on streams involving lead, zinc, copper, and nickel sulfides, as well as coal and industrial minerals. It has been applied as well to the removal of fine organic droplets from solvent extraction liquors.

In this chapter, a brief overview of antecedents to the Jameson cell is given. The general principles of operation are discussed, together with a

description of the various phenomena that take place in the downcomer. The effect of the operational variables on cell performance follows, including some data from operating cells.

II. DEVELOPMENT

The cell was devised in the period 1985–1986, when the inventor was undertaking a collaborative research project at Mt. Isa Mines Limited, Mt. Isa, Queensland. This is a large mine, accustomed to using the best modern practices in the production of copper, lead, and zinc concentrates. A number of large flotation columns were being designed and introduced at the time in the copper and lead/zinc circuits. Although it was clear that the columns would offer significant advantages over the conventional mechanical cells in terms of the ability to wash the froth, it was also clear that the collection process was very slow, necessitating large residence times and consequently the large columns, which have become a familiar feature of this technology. Accordingly, alternative methods of bringing the particles and the air into contact were investigated. Following initial work in the laboratory at Newcastle University, prototypes were tested and further developed in the concentrator at Mt. Isa, resulting in a production-scale design. A number of Jameson cells were installed in the lead circuit and in the nearby Hilton concentrator then under construction. Further cells were installed in a coal operation at Newlands, Queensland, and on a copper stream at the Peko Warrego mine, Tennant Creek, Northern Territory, Australia.

The use of columns as gas–liquid contactors, as well as the use of plunging jets to entrain air, has been previously tried in a number of designs, dating from the time of the first introduction of flotation in mineral processing. Perhaps the first to appear in the patent literature is the column described by Norris (2) in 1907, in which air appears to be both dissolved and entrained into a stream of pulp, which is then introduced to the bottom of a flotation column complete with froth crowder. Various devices for entraining air into a pulp by means of a plunging jet are described by Taggart (3) as "cascade machines." None of those early machines was capable of control of the air and bubble sizes, and it is apparent that they were designed more by guesswork than from basic principles of fluid mechanics. A review of alternative flotation machines has recently been given by Jameson (4).

In the design of the Jameson cell, it has been possible to take advantage of the many advances that have been made in the dynamics of single bubbles and of two-phase bubbly flows. Thus the jet entry conditions are such as to make micro-bubbles of controlled size, so as to create a large surface

area and hence to maximize the collection process in the downcomer. The downcomer is sized so that the bubbles created by the plunging jet are carried downward, but at the same time the downward pulp velocity is sufficiently low to allow bubbles to rise against the flow and create a mixture of high gas content. The downcomer diameter and the pulp flow must also be matched in such a way as to ensure that any large slugs that form are carried downward. In the froth zone, the rising velocity J_g of the gas must be such as to allow the froth to drain properly so that the gangue is not carried forward into the concentrate. At the same time, the J_g must be sufficiently high to minimize the drop-back of values and consequent loss of recovery. When washwater is used, the froth conditions must be such that again, the improvements in grade are not linked with reduction in recovery.

III. PRINCIPLES OF OPERATION

A. Introduction

In this section the different hydrodynamic regions occurring within the Jameson cell are discussed, with emphasis placed on the interactions between regions that determine the overall flotation performance. Before identifying the different hydrodynamic regions, however, it is useful to define the basic geometry of a Jameson cell and also to describe qualitatively what happens during startup and operation of a typical unit. As illustrated in Figure 1, the simplest geometry consists of a riser section, which is often referred to as the *cell*, and a single downcomer—although some of the larger units incorporate up to 30 separate downcomers in combination with a common riser section.

The downcomer consists of a vertical tube that is sealed at the top except for a regulated air inlet and a vertical nozzle through which the slurry feed is introduced. The base of the downcomer is located below the pulp level inside the riser. On startup, the air inlet at the top of the downcomer is closed, and the pulp feed is pumped through the nozzle. The air in the downcomer is entrained into the pulp, which forms the seal in the bottom of the cell; consequently, the pulp is drawn upward from the cell into the downcomer. The pulp level reaches the tip of the nozzle quite quickly, and as a consequence of the hydrostatic suction developed by the head of this pulp, the pressure in the head of the downcomer is less than atmospheric. When the inlet is opened, air is drawn into the headspace at the top of the downcomer where it is entrained into the downcomer contents by the plunging jet. The entrained air is broken up into fine bubbles that are quickly dispersed into the pulp and carried downward by the bulk fluid motion.

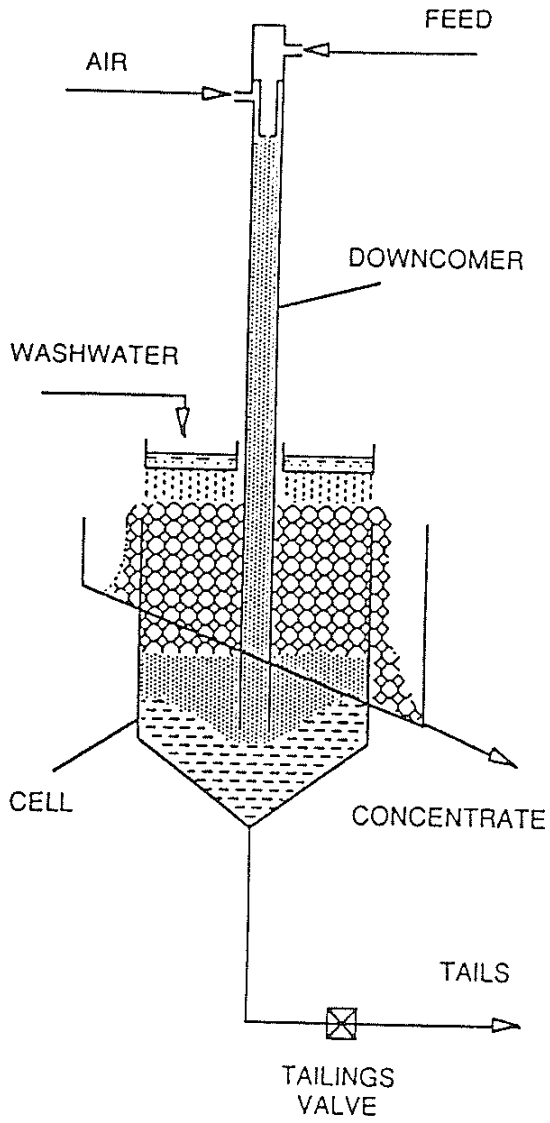

Figure 1 Layout of a single-downcomer Jameson cell.

The three-phase mixture passes from the base of the downcomer into the cell proper, which has a much greater cross-sectional area than the downcomer. Consequently, the downward superficial velocity of the mixture is reduced, allowing the particle-laden bubbles to disengage from the liquid, rise to the surface, and form a layer of froth. The froth then drains before overflowing into a collection launder, while the liquid phase and unrecovered particles leave through a valve at the base of the cell.

B. Hydrodynamic Regions

The different hydrodynamic regions that constitute the Jameson cell are shown in Figure 2. The free jet, submerged jet, mixing zone, and pipe flow zone occur within the downcomer, while the disengagement zone, which includes the froth layer, occupies the entire riser volume.

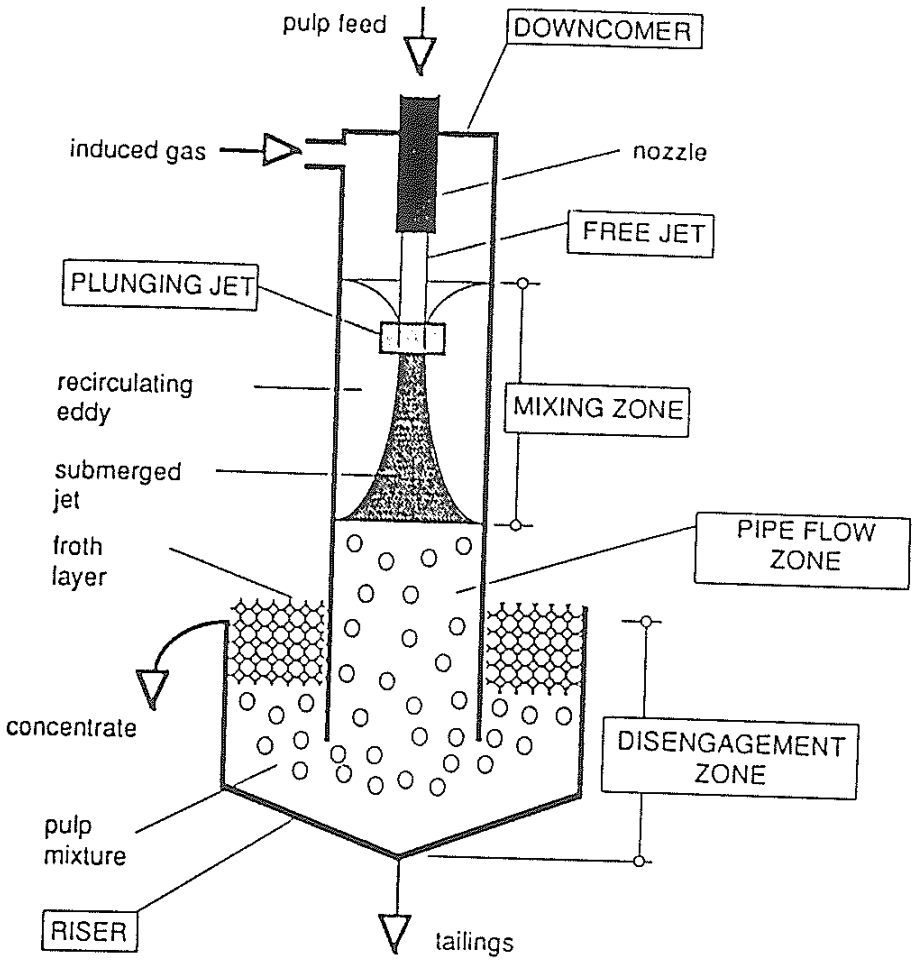

Figure 2 The various active zones in the Jameson cell.

1. Free Jet

The free jet is defined as the stream of liquid (pulp) feed between the tip of the nozzle and the horizontal free surface inside the downcomer. Once the jet leaves the nozzle, its diameter is determined by the relaxation of the velocity profile inside the jet and also by the interaction of the free surface of the jet with the surrounding atmosphere (5). The velocity relaxation inside the jet occurs as a result of the change from the velocity profile, when the pulp is inside the nozzle, to a plug flow velocity profile once the jet has left the confines of the nozzle. Further downstream the velocity profile changes from plug flow to parabolic flow due to the interaction of the outer boundary layer of the jet with the surrounding atmosphere. This interaction slows the velocity of the jet at its free surface resulting in an expansion in the free jet diameter.

Associated with the velocity relaxation within the jet once it leaves the nozzle is a lateral movement that creates undulations on the jet free surface (6). As shown in Figure 3, the undulations increase in magnitude with

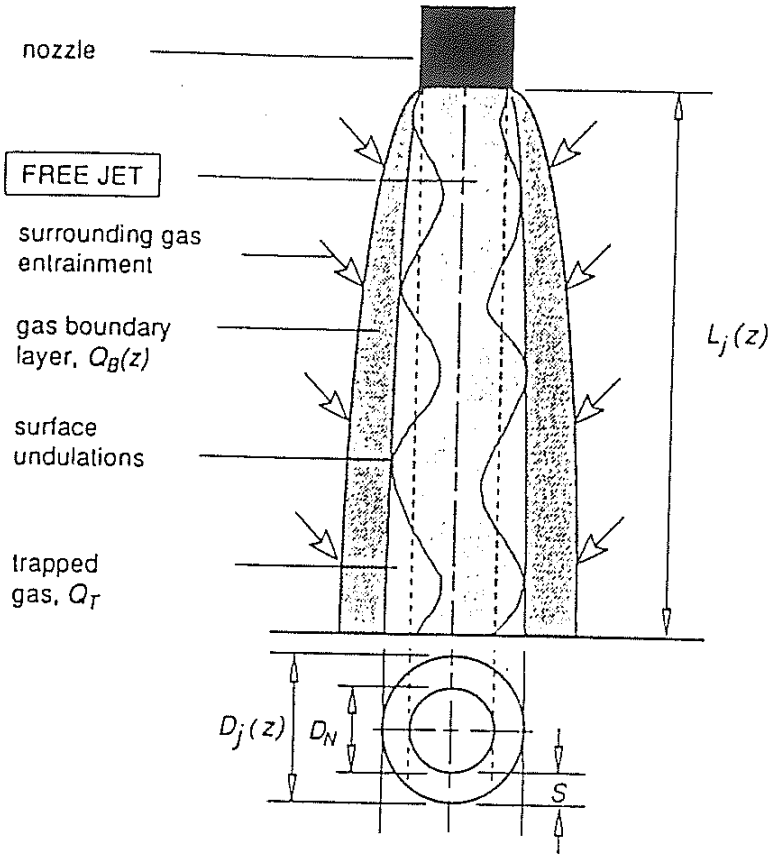

Figure 3 The mechanisms of air transport by a free jet.

increasing free jet length thereby increasing the effective diameter of the jet. The irregular nature of the jet surface created by the undulations is often called the *surface roughness*, and jets that exhibit this characteristic are called *rough jets*. Jets that display no surface roughness—and are generated using specially designed nozzles—are called *smooth jets*.

The surface roughness S is defined in Figure 3 as the difference between the nozzle diameter D_N and the effective diameter of the jet $D_j(z)$, which is a function of the length of the free jet $L_j(z)$. The surface roughness is strongly influenced by the upstream conditions of the jet delivery system. Disturbances such as swirl generated by a pump, vibration from a motor, or irregularities on the inside surface of the pipework are all amplified once the pulp passes through the nozzle, resulting in an increase in the surface roughness.

Also illustrated in Figure 3 is the transport of air by the free jet as it passes through the headspace at the top of the downcomer. First, a thin annular boundary layer of air $Q_B(z)$ is carried along adjacent to the jet free surface. Second, a quantity of air Q_T is trapped within the effective diame-

ter of the jet. Therefore, the total amount of air transported by the free jet Q_F can be written as

$$Q_F = Q_B(z) + Q_T \tag{1}$$

Smooth jets that exhibit no surface roughness have no trapped air component. Hence, for two jets with the same velocity and pulp flow rate, a rough jet transports a greater volume of air than a smooth jet. Usually this results in a greater air/feed ratio Q_G/Q_L into the downcomer—where Q_G and Q_L are the air and liquid volumetric feed rates into the downcomer, respectively—which leads to higher air void fractions and interfacial areas. Therefore, it is desirable to operate the Jameson cell using rough jets, a situation that is not difficult to reach in practice since the jets normally have rough surfaces created by the disturbances generated within the delivery system.

2. *Plunging Jet*

The plunging jet is defined as the region where the free jet impacts with the horizontal free surface at the top of the downcomer, resulting in air entrainment. At the point of impact, a depression is formed in the horizontal free surface, which is often referred to by McCarthy (6) as the *induction trumpet*. A half-sectioned profile of the induction trumpet is illustrated in Figure 4, which shows the free surface at the top of the downcomer being drawn downward by the momentum of the free jet. The induction trumpet has a wide opening at the top, which tapers down to a thin annular film adjacent to the effective boundary of the free jet. The fluted entrance channels the moving air boundary layer into the induction trumpet, and a portion of it Q_f enters the thin film, while the remaining air inside the boundary layer Q_U travels radially out along the horizontal free surface and returns to the headspace (7).

The induction trumpet periodically collapses due to instabilities generated on its free surface, resulting in entrainment of the annular film. Combining this quantity with the air trapped within the effective jet diameter at the point of impact, the total entrainment rate of the plunging jet Q_E is

$$Q_E = Q_f + Q_T \tag{2}$$

It should be noted that the entrainment capacity of the plunging jet given by Equation (2) is not equivalent to the air feed rate into the downcomer. The reason is that air is being continuously circulated within the mixing zone, and a portion Q_H returns to the headspace, from which it is reentrained by the plunging jet. The air recirculated from the mixing zone effectively reduces the amount of new air Q_G that can enter the downcomer.

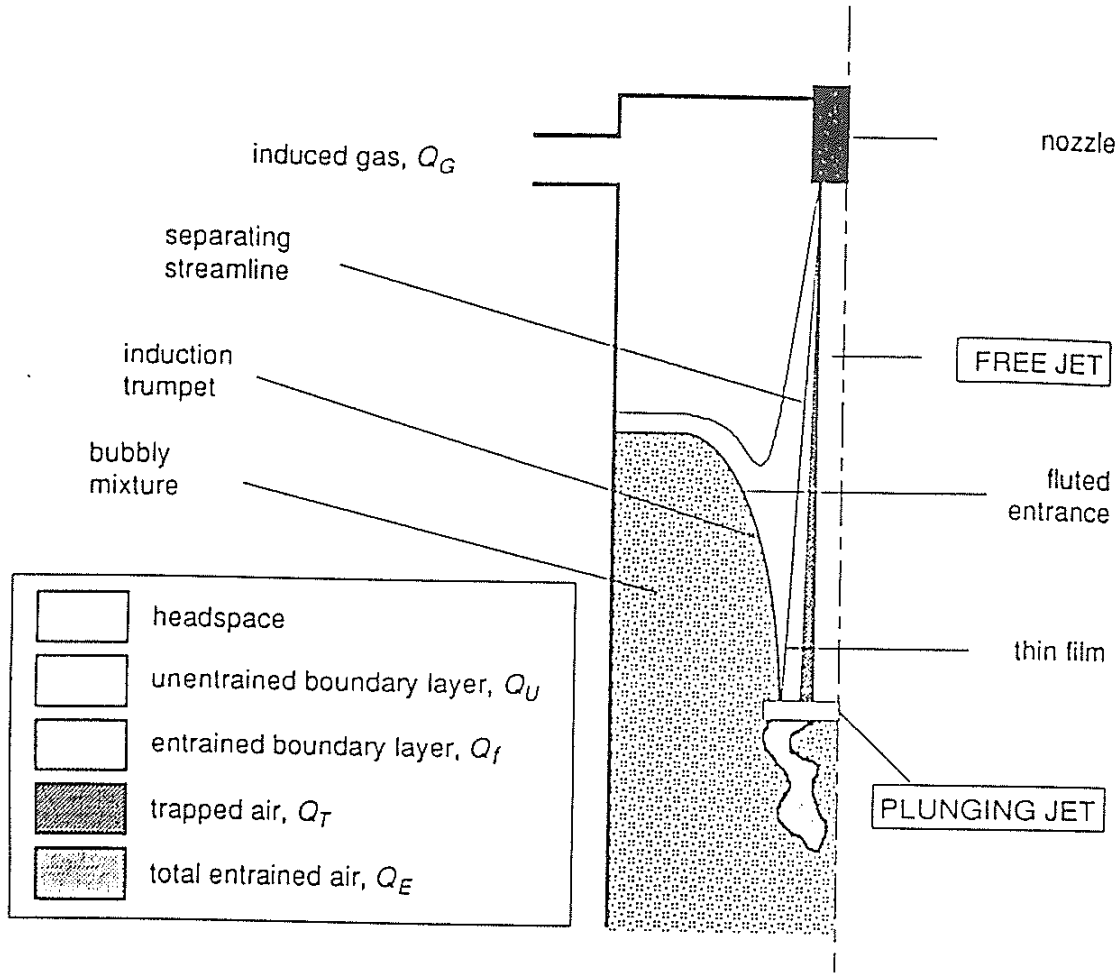

Figure 4 Components of air flow into plunging jet.

3. *Mixing Zone*

The mixing zone is defined as the volume occupied by (1) the fluid inside the submerged jet immediately below the plunge point that expands to occupy the cross-sectional area of the downcomer and (2) the body of fluid recirculating between the submerged jet boundary and the column wall—often referred to as the recirculating eddy. The high velocity gradients between the submerged jet and the recirculating eddy result in high energy dissipation rates within the mixing zone, which are responsible for the breakup of the air once it is entrained by the plunging jet. The entrained air is broken into fine bubbles before being transported downward into the pipe flow zone by the bulk fluid motion.

The size of the bubbles produced inside the mixing zone is related to the forces acting on the bubble surface. In low viscosity fluids, like those normally encountered in flotation circuits, the bubbles are deformed by forces arising from liquid velocity fluctuations acting over distances of the order

of the bubble diameter. The restoring force resisting the deformation of the bubble is due to surface tension acting at the air–liquid interface. The ratio of these forces is known as the Weber number *We* and is defined as

$$We = \frac{\rho_L \overline{u^2} d}{\sigma} \tag{3}$$

where $\overline{u^2}$ is the average value of the squares of the velocity differences acting over a distance of the order of the bubble diameter d, and ρ_L and σ are the liquid (pulp) density and surface tension, respectively. If the bubbles are small compared to the turbulent macroscale but large compared to the microscale, the velocity fluctuations, following Hinze (8), can be related to the energy dissipation rate per unit volume $\dot{E}$ by the relationship

$$\overline{u^2} = C_1 \left(\frac{\dot{E} d}{\rho_L}\right)^{2/3} \tag{4}$$

where $C_1 \approx 2$ according to Batchelor (9).

For a given bubble size and at low Weber numbers, the deformation forces are dominated by the restoring forces, and the bubble is stable. However, as *We* increases, the shape of the bubble becomes increasingly distorted. Eventually a critical Weber number We_c is reached where the bubble becomes unstable and breaks up into smaller bubbles. The maximum bubble size d_m corresponding to the critical Weber number is

$$d_m = \left(\frac{We_c}{2}\right)^{3/5} \rho_L^{-1/5} \dot{E}^{-2/5} \tag{5}$$

Equation (5) has been used by Evans et al. (10) to predict the maximum stable bubble diameter inside the mixing zone, using estimates of the critical Weber number and the energy dissipation rate per unit volume.

The volume of the mixing zone is determined by the point of contact of the expanding jet and the wall of the enclosing downcomer. By considering the radial flow of momentum from the incoming jet to the recirculating eddies in the mixing zone, Evans (11) derived the following expression for the half angle β subtended by the expanding jet at the virtual origin:

$$\tan\beta = \frac{D_d}{L_{MZ}} = \eta \left(\frac{P_1}{\rho_L U_j^2}\right)\left(\frac{\rho_{MZ}}{\rho_L}\right)\left\{\frac{(0.37(R_c^2 - 0.5 R_j^2))^{0.5} - 0.64 R_j}{R_j}\right\}\left\{\frac{U_j - U_{e,max}}{U_j}\right\} \tag{6}$$

where η is a jet energy transfer efficiency found by experiment to be 0.089, ρ_{MZ} is the density of the two-phase mixture in the mixing zone, R_c and R_j

are, respectively, the downcomer and jet radius, P_1 is the pressure in the headspace at the top of the downcomer, U_j is the jet velocity, and $U_{e,max}$ is the maximum return velocity in the eddy, which has been found by experiment to be 0.085 U_j.

The volume of the mixing zone is then assumed to be the volume enclosed by the cylinder formed by the downcomer of internal diameter D_d and the length L_{MZ} of the mixing zone.

Evans et al. (10) have compared the sizes of bubbles predicted by Equation (5), with measurements of the sizes of bubbles formed in an air water system, and found agreement within ±20%. Two downcomers of diameters 44 mm and 74 mm were used, and the jet velocity varied from 7.8 to 11.53 m/s. The bubble sizes were generally in the range 200–400 μm.

4. *Pipe Flow Zone*

The pipe flow zone is the region below the mixing zone inside the downcomer. The flow here resembles the downward flow in a vertical pipe. At low air flow rates, bubbly flow exists in which small discrete bubbles of different diameters move downward with the bulk liquid flow but not generally with the same velocity as the liquid phase. If the air flow rate is increased, the discrete bubbles coalesce and alternating air and liquid regions, or slugs, form inside the downcomer. The air slugs or Dumitrescu bubbles (12) have hemispherical caps that occupy nearly the entire cross-sectional area of the downcomer. The rise velocity U_r of these bubbles is a function of the downcomer diameter D_d and g, the acceleration due to gravity:

$$U_r = 0.496\left(\frac{gD_d}{2}\right)^{1/2} \tag{7}$$

At air flow rates when the Dumitrescu bubbles are initially formed, the drag and viscous forces are sufficiently great to give the bubbles a net downward velocity, and they are carried out through the base of the downcomer. However, if the air flow rate is further increased, the Dumitrescu bubbles become elongated, and the shearing forces present in the liquid make them unstable. This results in a chaotic mixture of air and liquid pockets known as churn-turbulent flow.

In terms of flow characteristics for the pipe flow zone, bubbly flow is the most desirable because it produces the greatest collection area for a given air/feed ratio, and it also provides for stable Jameson cell operation. With churn-turbulent and slug flow, the surface area per unit of gas volume is very low, and the collection efficiency is significantly reduced. Moreover, there is a much greater tendency for larger bubbles, with rise velocities greater than the net downward motion, to return to the top of the down-

comer and be reentrained by the jet, reducing the amount of new air that can be introduced, and hence reduces the effective air/feed ratio.

5. *Disengagement Zone*

When the bubbly mixture reaches the bottom of the downcomer, it passes out into a vessel of larger cross-section, and the bubbles then disengage from the main pulp flow. For efficient action, the base of the downcomer is below the liquid level in the cell proper, and a hydraulic seal is maintained. Because of its low effective density, the bubbly flow initially hugs the outer wall of the downcomer, but as it rises it tends to entrain slower-moving fluid and then spreads laterally. The bubbles rise relative to the liquid and pass from the pulp layer into the base of the froth layer. The processes taking place in the froth are very important in the determination of the overall grade and recovery. If the gas superficial velocity J_g is too small or the froth depth too large, the bubbles coalesce and the froth degrades, leading to squeezing of the least hydrophobic particles and loss of recovery. If on the other hand the air rate is too high and the froth depth too shallow, the recovery may be high but at a low grade due to entrainment of gangue. Consequently, the cell must be operated to give optimum grade and recovery by manipulating the air rate and froth depth. If the air rate is too high altogether, the cell may "flood." This phenomenon occurs when the upward gas velocity exceeds the rate at which the liquid can drain back into the pulp layer and is evidenced in practice by the production of a very wet froth. In fact, when the cell floods, there is no distinction between the froth and pulp phases, and the interface that normally exists between them is lost. The phenomenon of flooding has been investigated in several recent papers. Pal and Masliyah (13) have given an empirical equation for the critical flooding velocity, and Langberg and Jameson (14) have given a more basic description, relating the flow in the froth and pulp phases to the flow of liquid in a packed bed, where in the present case the packing consists of the bubbles. Xu et al. (15) have given a comprehensive account of the various flow regimes and methods for calculating the limiting flow rates.

Washwater can be used with the Jameson cell as with other flotation columns, when high-grade products are required. In some cases it is possible to achieve the grades required by proper design of the cell, regarding the typical J_g allowed for, and by controlling the froth depth. However, the use of washwater adds another control variable of great power, whose proper use can lead virtually to total flushing out of the entrained gangue. The use of washwater does not unduly complicate the analysis of the flow presented in Refs. 13–15, and the same principles apply. The washwater flow is sometimes used to control liquid level as well as to wash the froth,

but this practice seems to have nothing to recommend it and should be avoided as it adds further complexity, especially when the water flows needed for level control purposes are such as to be in conflict with optimum metallurgical conditions in the froth, for best grade and recovery.

The liquid layer in the cell forms a complex system of liquid and air recirculation patterns of varying turbulence and void fraction. The cell design is based on downcomer flows and downcomer placement to optimize this system to produce best grade and recovery. There is no limit on its volume, provided the net downward velocity of the pulp J_L is sufficiently low to avoid the entrainment of bubbles in the underflow. When the froth and disengagement zones have the same cross-sectional area, the two important velocities are the rate of rise of the bubbles in the pulp, and the rate of drainage of liquid in the froth. The former is usually greater than the latter, so that a column sized to give the correct J_g will also give the correct J_L, and bubble entrainment in the downward flow will not be a problem.

C. Interactions and Operating Stability

The interactions taking place between regions inside the Jameson cell and the various recycle paths taken by the air are illustrated by the flowchart shown in Figure 5. The performance of the cell is determined principally by the collection rate of the bubbles inside the downcomer and to a lesser extent by the separation of the product from the tailings stream in the riser. In general, for a given cell cross-sectional area, the collection rate is increased by increasing the air/feed ratio into the downcomer. However, an increase in this ratio can also lead to instabilities and in some cases to the complete collapse of the system. The operating stability of the Jameson cell as a function of air feed rate is shown in Figure 6.

At low rates of air induction, the level inside the downcomer is sustained just below the level of the nozzle, indicating that the plunging jet can effectively entrain all of the air in the headspace. The air is dispersed into very fine bubbles, which are carried downward by the net fluid movement, resulting in minimal recirculation of air back into the headspace from the mixing zone. In general, this is the ideal mode of operation as it provides (1) the most stable operating condition, (2) very small bubbles, and (3) the longest residence time inside the downcomer, thereby maximizing the bubble-particle contact time. The only disadvantage with this operating mode is the relatively smaller air/feed ratio inside the downcomer, which may lead to lower rates of production of interfacial area. (Recent unpublished work has shown, however, that in some practical cases a reduction in the ratio is compensated directly by the reduction in bubble size and hence an increase in the surface area of interface produced by a given volume of

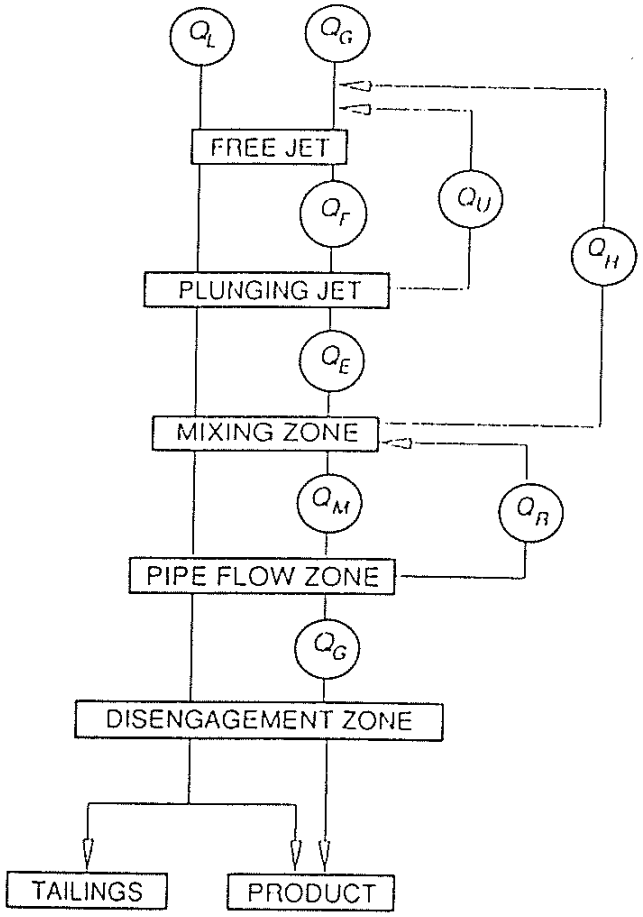

Figure 5 Interaction paths in the Jameson cell.

air. Thus a reduction of air rate, which gives much more stable downcomer operation, does not necessarily lead to a reduction in recovery, providing the J_g is maintained constant.)

If the air rate is increased, a point is reached where the jet can no longer entrain all of the air being introduced into the headspace, and the froth level in the downcomer starts to drop. Fortuitously, it appears that some type of compensatory phenomenon is at work. This phenomenon has the effect that the rate of entrainment of air by the plunging jet increases up to a point, as the length of free jet increases. The phenomenon is possibly linked to the increase in the effective jet diameter with increase in the free jet length. Whatever the reason, a new equilibrium height is reached inside the downcomer, marking the length where the jet can effectively entrain all of the entering air. In a sense the jet is self-regulating in that the length of the free jet will increase to accommodate the increase in the amount of air added to the downcomer (up to a point).

An increase in the free jet length also leads to (1) a reduction in the froth height inside the downcomer, resulting in a reduction in the residence time

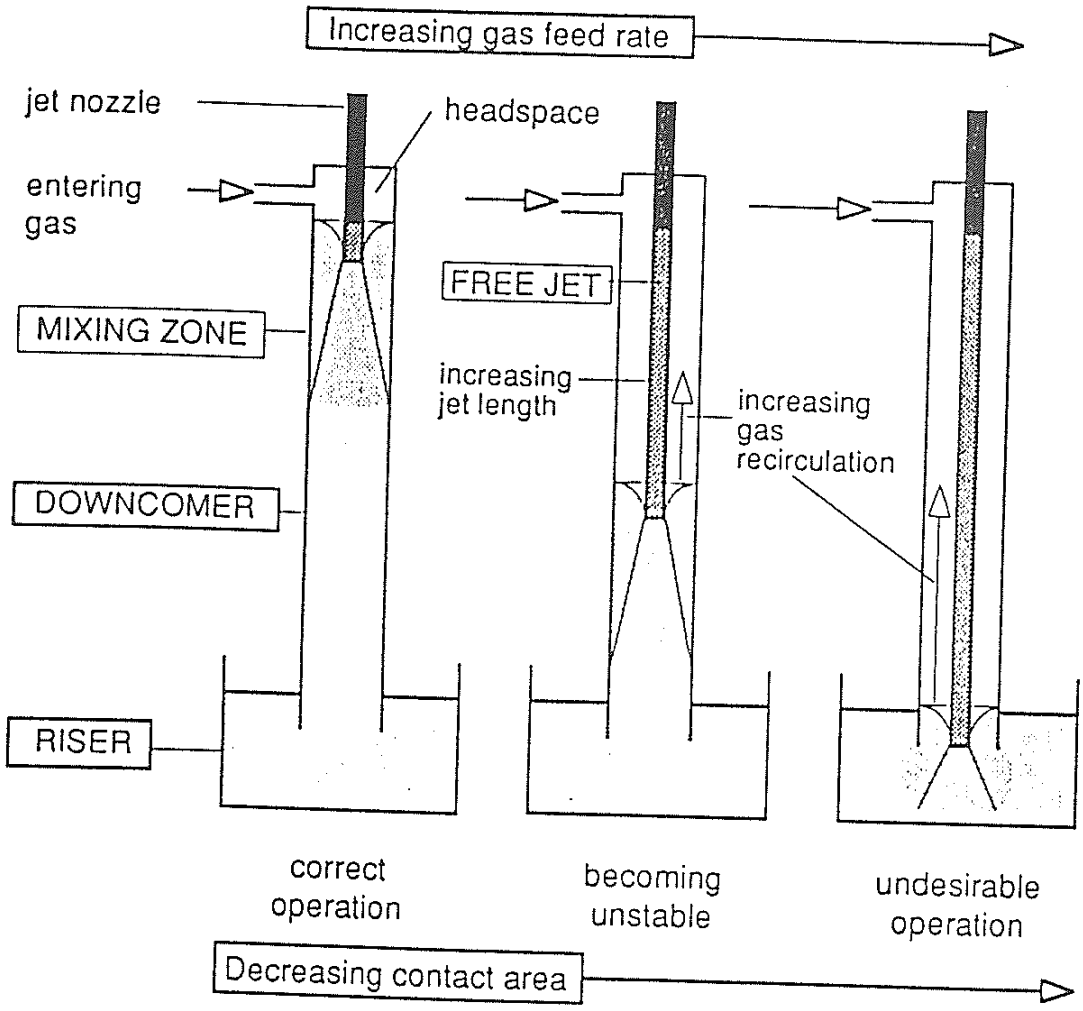

Figure 6 Variation of downcomer operation with airflow rate.

of the bubbles, and (2) an increase in mean bubble size generated within the mixing zone (11), resulting in a decrease in the amount of interfacial area generated per volume of air inside the downcomer.

More important than the potential loss in recovery rate is the possible effect of increasing the air feed rate on the overall stability of the system. At very high air rates, bubble coalescence results in the formation of large gas slugs in the pipe flow zone, which restrict the flow of air through the downcomer. This leads to an increase in the pressure in the headspace causing a drop in the froth level and, in the extreme case, the complete collapse of the system.

D. Conditions in the Downcomer

A number of investigators have studied the void fraction and gas holdup in the downcomer. Sanchez-Pino and Moys (16) measured the hydrostatic

pressure between two points in a vertical downcomer and used a drift-flux method to analyze the data. The void fraction or gas holdup varied from 20% at an air/feed ratio of 0.1 to 55% at a ratio of 0.9. Marchese et al. (17,18) used a conductometric technique to measure the void fraction in the downcomer and compared their results with those from a total isolating method in which the contents of the downcomer are trapped between two valves in-line, which are closed simultaneously.

The values they obtained can be contrasted with those found in conventional columns that are typically of order 15%. The high void fractions explain the extremely rapid kinetics found in the downcomer; the values suggest that the bubbles are in fact approximating the close-packed spherical limit and that it would be unrealistic to expect void fractions in excess of 55 to 60%. Void fractions above 60% have been observed, but the most likely explanation is that the contents of the downcomer then consist of a dense foam of average void fraction 55 to 60%, embedded in which is a small number of relatively large slugs or Dumitrescu bubbles, which would contribute virtually nothing to the collection processes in the froth.

IV. JAMESON CELL OPERATING PARAMETERS

Some general operating characteristics of the Jameson cell are now discussed.

A. Froth Depth

The froth phase produced in a Jameson cell can be controlled in the same manner as in conventional columns. Shallow froth depths (less than 200 mm) are used where high recovery is necessary and grade is of secondary importance, while deeper froths (up to 1000 mm) are employed to obtain maximum concentrate grade. Shallow froths result in significant entrainment of very fine (less than 10 μm) gangue mineral components that accompany the pulp phase. Use of deeper froths results in significant drainage of hydrophilic gangue producing a higher grade concentrate and a higher percentage of solids in the concentrate. Under some circumstances, addition of counter-current froth washwater assists froth mobility, where otherwise excessive froth drainage would result in an immobile froth.

B. Superficial Gas Velocity

The superficial gas velocity J_g (cm/s) is the upward superficial velocity of air in a flotation cell. In the Jameson cell, the J_g is calculated by dividing the downcomer air rate (cm^3/s) by the cross-sectional area (cm^2) of the riser part of the cell. The cell is normally circular or rectangular in section, and

the appropriate cross-sectional area is simply the area normal to the direction of the flow of the froth, excluding the area occupied by the downcomer(s). It is conveniently expressed in units of cm/s because values typically range from 0.5 to 4 cm/s in practice.

For a stream that is not carrying-capacity limited (see Sec. IV.H), the recovery and concentrate carrying rate (g/min/cm^2) tend to increase with increasing J_g, as in conventional columns (see Refs. 19 and 20). For a given stream and frother concentration, a maximum air rate (subsequently $J_{g,max}$) is reached, above which froth flooding occurs, resulting in the loss of froth-pulp interface, a very wet froth, and total loss of selectivity. In flooding, the entire cell fills with froth as the only stable phase, and there is no pulp phase.

Some data of interest are shown in Figure 7 for a lead/zinc circuit. Data were obtained using a Jameson cell in parallel with a conventional column. In each case, it is seen that there is a strong correlation between the production rate of solids and the superficial gas velocity J_g. For a given air rate, the Jameson cell gives greater production rates than the column, presumably a consequence of the smaller bubbles generated in this device.

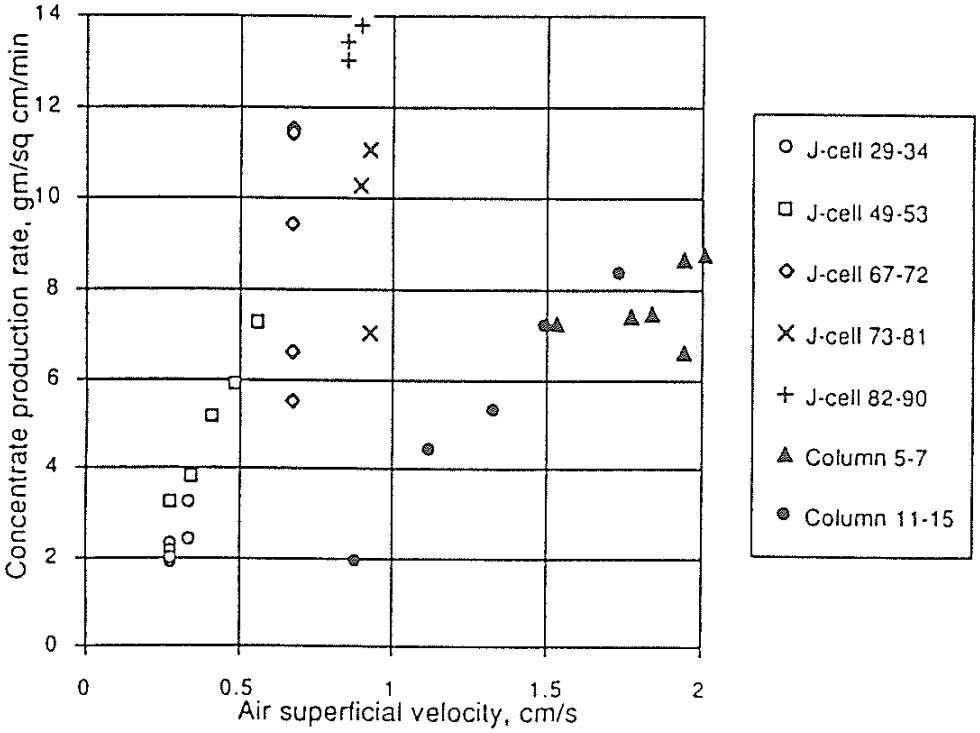

Figure 7 Variation of concentrate production rate with superficial air velocity J_g, for a lead/zinc flotation, with a conventional column and a Jameson cell in parallel. The spread in data is due to variations in froth depth. The numbers in the legend refer to various test runs.

The operating J_g used in the sizing of the Jameson cell depends strongly on the application, and on the residual reagent concentrations from any upstream processes. Generally speaking, low values (J_g = 0.4 to 0.8 cm/s) are employed in cleaning applications, and high J_g's (1.0 to 2.0 cm/s) are employed in roughing or scavenging applications. The reasons for these choices are as follows. In cleaning operations, a high proportion of the feed reports to the concentrate, and the froth loading tends to be high. Consequently, the bubbles are well coated with particles, which tend to stabilize the froth. The drainage rate of the interstitial liquid in the froth is retarded by the relatively high concentration of particles, so it is necessary to design for lower values of J_g to allow time for the gangue to drain from the froth to obtain the required high grade. In roughing applications, however, only a small fraction of the feed reports to the concentrate, and the froths formed tend to be less stable as a consequence. Also, gangue entrainment is not such a serious problem, because it can be coped with in the downstream cleaning circuit. In order to maintain a stable froth, it is therefore usual to design a Jameson cell for a roughing application with a higher J_g than in the cleaners.

In some circumstances, high residual concentration of reagents in the feed necessitates the use of low J_g's to avoid froth flooding. Although frother concentration is of primary importance to bubble size and hence the advent of froth flooding, circumstances have risen where collector (xanthate) and frother (methyl isobutyl carbinol, MIBC) interaction has been observed (21). In such a case, the frother dose should be decreased if the collector dose is increased, and vice versa. Too high a frother or collector concentration can lead to froth flooding, while too low a dose can lead to loss of froth stability.

Particle size can also have an influence on the maximum J_g, due to its effect on froth stability through bubble bridging. Small particles (less than 100 μm) are easily collected at low gas rates (J_g less than 1.0 cm/s), while recovery of coarser particles (greater than 100 μm) may be assisted by higher rates (J_g greater than 1.0 cm/s).

C. Bubble Size

Bubble sizing determinations for full-scale operating cells and test cells at the University of Newcastle show that the Jameson cell produces an arithmetic mean bubble diameter of the order of 300–600 μm, while the Sauter (volume-to-surface) mean diameter d_{vs} is of order 360–950 μm (21). These sizings compare very favorably with conventional columns where the Sauter mean bubble size is typically 2 to 3 mm.

Figure 8 shows bubble size versus air/feed ratio for a 300-mm diameter

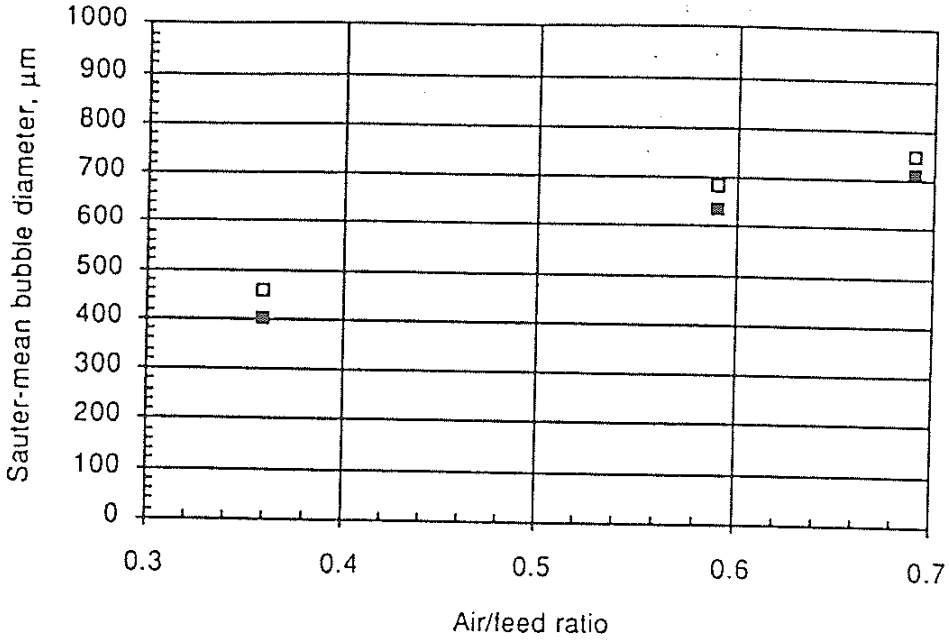

Figure 8 Measured values of the Sauter mean bubble diameter in exit stream from a Jameson downcomer as a function of the air/feed ratio, in flotation of a copper retreatment stream. Results for two separate determinations are shown.

Jameson pilot cell treating a fine copper retreatment stream (d_{80} = 30 μm). These data confirm visual observations that bubble size decreases with decreasing air/feed ratio.

Chatiar (22) carried out experiments in the laboratory using air and water with MIBC as frother and found that as the concentration increased, the mean bubble size was reduced, up to a concentration of 30 ppm V/V, beyond which there was little change.

D. Air/Feed Ratio

Jameson cells generally operate with a volumetric air/feed ratio of 0.3–0.9. Experiences with large (2–3 m diameter) Jameson cells indicate that operation at a low air/feed ratio does not appear to detract from metallurgical performance *providing the superficial gas velocity J_g is maintained* above a certain minimum value. Operation at lower air/feed ratios has a stabilizing effect producing a more uniform and finer bubble size. A significant advantage of operation at lower air/feed ratios is that lower concentrations of frother are required.

Maintenance of metallurgical performance at low air/feed ratios can be explained by considering the flux of interfacial area S_b (interfacial area/s) per unit of column cross-sectional area (s^{-1}) as defined by Finch and Dobby (19):

$$S_b = 6\frac{J_g}{d} \tag{8}$$

where d is the bubble diameter. The superficial bubble surface rate (and hence the collection capability) can be maintained with reduced superficial gas rate providing the bubble size decreases accordingly. The data in Figure 9 were calculated using information from Figure 8 using Equation (8) and show the superficial bubble surface rate as a function of the air/feed ratio for a fixed cell cross-sectional area. It is seen that the superficial bubble surface rate remains almost constant at 55 s^{-1} approximately, despite two-fold changes in the air/feed ratio.

E. Washwater Ratio

The washwater ratio is defined as the ratio of the washwater addition rate to the flow rate of water in the concentrate:

$$W = \frac{Q_{WW}}{Q_{WC}} \tag{9}$$

where Q_{WW} is the washwater flow rate and Q_{WC} is the rate of flow of water in the concentrate. The washwater ratio is a relative measure of the amount of washwater applied.

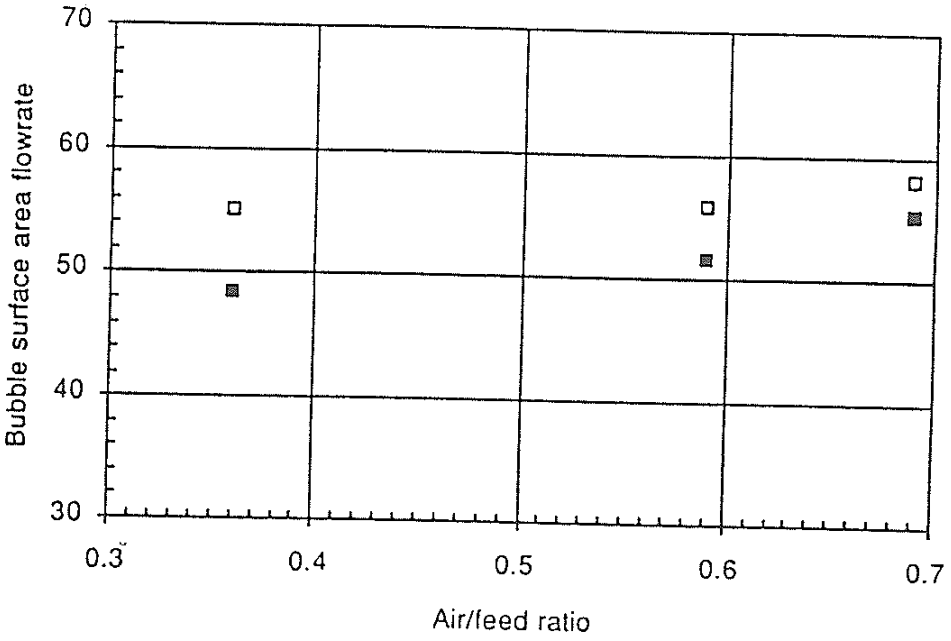

Figure 9 Flux of interfacial area for bubbles generated by downcomer and passing into the froth phase at the air/feed ratios shown in Figure 8. The interfacial flow rate S_b is calculated from Equation (8). The drop in airflow rate at low values of the ratio is mainly compensated by a corresponding decrease in the mean bubble size.

Another common method of describing the washwater addition is in terms of the bias, that is, the absolute excess of the washwater applied over the quantity of water being recovered in the concentrate, expressed as a superficial velocity J_b (cm/s):

$$J_b = \frac{Q_{WW} - Q_{WC}}{A_C} \tag{10}$$

where A_C is the cross-sectional area of the column. If no washwater is used, the washwater ratio is zero, and the bias is negative. When $J_b = 0$, $W = 1$; positive bias corresponds to washwater ratios greater than unity.

Although the bias does give an indication of the absolute amount of washwater being added, its use can be misleading because it does not take into account the wide variation in the absolute values of the rate of water entrainment in the concentrate. It is preferable to use the washwater ratio, which is a relative figure.

Consider, for example, a rougher application in which the mass flow of recovered solids is only a small fraction of the feed. In such a case, the flow of concentrate will be low and a correspondingly low volume of washwater will be needed to replace the water being carried out of the cell in the concentrate. Thus good froth washing may be achieved with a relatively low positive bias, say 0.005 cm/s. On the other hand, in a cleaning operation, where the mass flow of concentrate is high, a much higher superficial flow rate of washwater would be needed to replace the water in the concentrate, since there is much more water being removed in the froth.

Figure 10 shows a comparison of measured washwater ratios and bias rates for a range of operating conditions for a Jameson cell operating on a zinc rougher application. Although the bias covers a relatively narrow range, the washwater ratio has much greater variation. To an operator, the difference in bias between 0.02 and 0.04 cm/s may seem negligible, but it can be seen that in some circumstances, such changes in J_b may lead to a threefold increase in the washwater ratio—supplying in effect a 200% overload of washwater.

Although it might be thought that a cell should be operated with $W > 1$, there is evidence to show that the optimum operating value should be in the range 0.5 to 1. Figures 11 and 12, for example, show the effect of washwater ratio on recovery and grade, respectively, of a fine copper retreatment stream ($d_{80} = 30$ μm). As the washwater ratio is increased, the recovery decreases significantly up to $W \approx 1$ and then decreases more gradually for $W > 1$. The grade increases progressively up to a washwater ratio of 1.0, but no further grade improvement is observed at washwater ratios above this value. These data, together with other Jameson cell operating

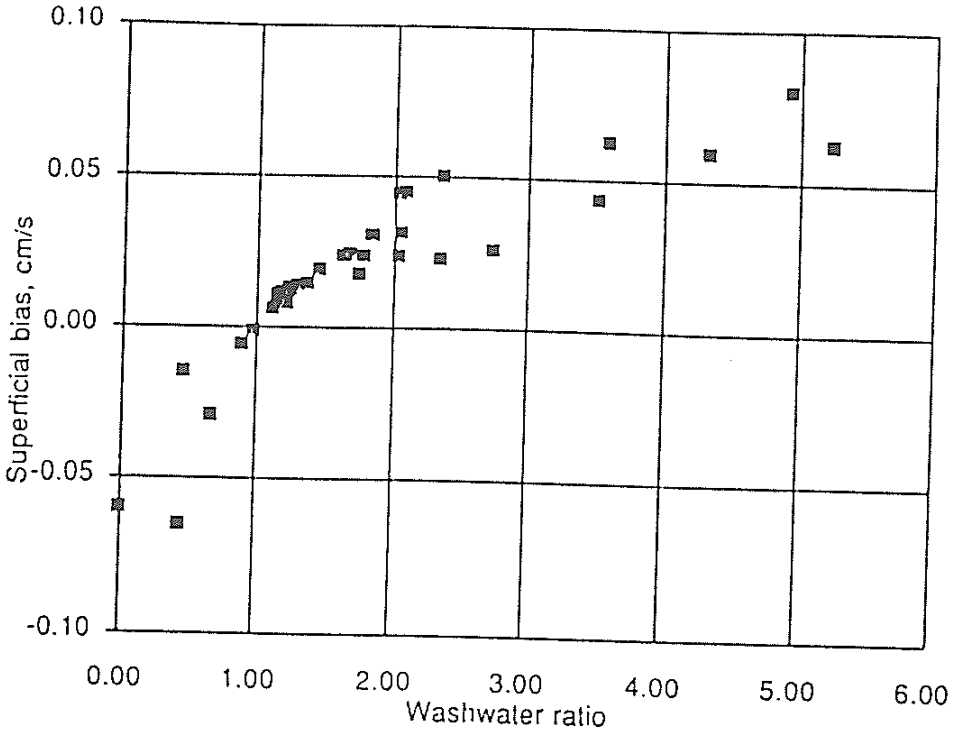

Figure 10 Plot of superficial washwater bias J_b against the washwater ratio calculated for the same zinc rougher flotation runs. Note the large variation in washwater ratio for relatively small changes in the absolute bias.

data, confirm that the best washwater operating point is at a washwater ratio of slightly less than unity, where recovery and grade are both high. Higher washwater addition simply results in decreased recovery without compensating improvements in grade. Precise on-line washwater bias measurement is highly desirable in order to maximize recovery at required grade.

F. Reagents

In streams tested to date, MIBC, long-chain alcohols, polyglycol propylenes, and polyglycol ethers have been used as the frothers in the feed to the Jameson cell, usually in the range 5 to 25 ppm. In cleaning applications, generally no frother addition is required due to the residual concentration from the roughing stage. In some cases, excessive frother from the upstream stage can lead to a reduction in maximum superficial gas rate J_g, which can be applied in the Jameson cell. Froth flooding is initiated at lower air rates due to the finer bubble size generated by an excess frother concentration (see Ref. 19, p. 22).

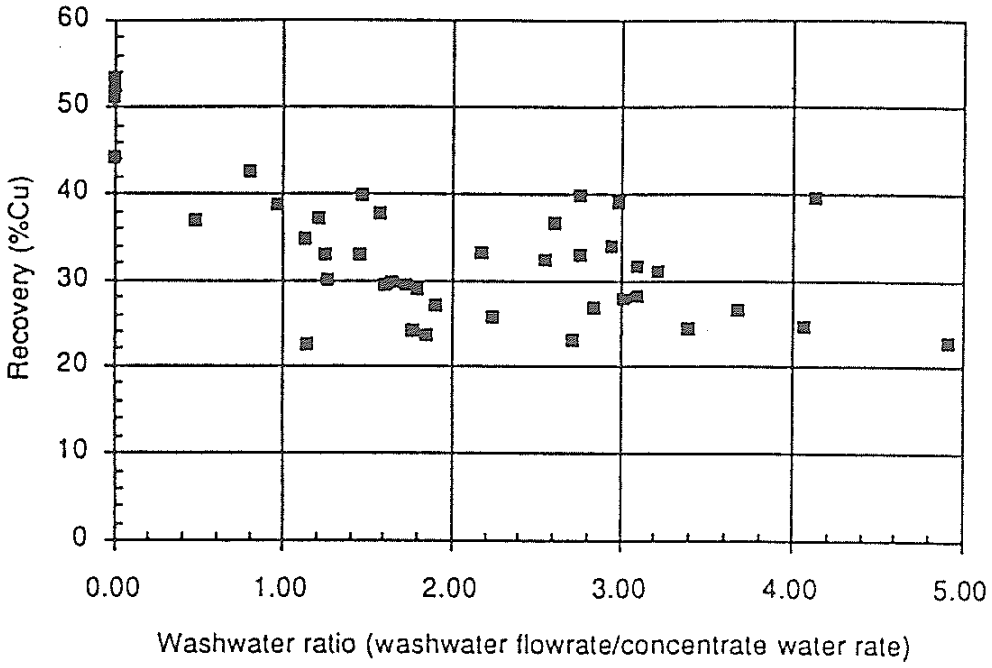

Figure 11 Effect of washwater ratio on recovery in the flotation of a copper retreatment stream. The apparent scatter here and in Figure 12 is due to differences in flotation conditions between individual runs, particularly in the froth depth and air rate. Note that the progressive decline in recovery as washwater is increased.

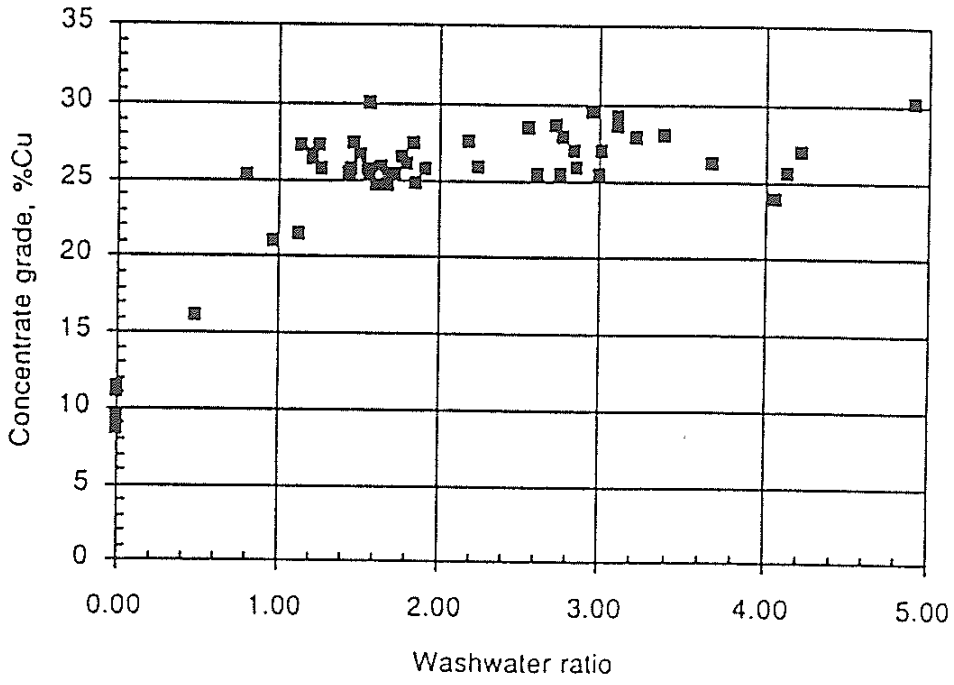

Figure 12 Grade vs. washwater ratio in flotation of a fine copper retreatment stream. The grade increases markedly until the washwater ratio reaches a value of 1 approximately and thereafter remains constant.

G. Downcomer Void Fraction

Experimental studies by Evans (11) and Marchese et al. (17,18) have shown that the void fraction (gas holdup) in a Jameson downcomer is generally in the range 50 to 60% by volume.

The downcomer void fraction can be measured directly, either from the isolating technique or from conductivity measurements. It can also be calculated using a downcomer momentum balance.

The gas void fraction ϵ in the dense foam inside the downcomer is defined as

$$\epsilon = \frac{V_G}{V_G + V_L} \tag{11}$$

where V_G and V_L are the volumes occupied by the gas and liquid (pulp) phases, respectively. In the isolating method, the contents of a section of the downcomer are trapped between two valves that are closed simultaneously, thus allowing direct measurement of V_G and V_L.

With the conductometric method, use is made of classical potential theory to relate the measured conductivity to the voidage. Thus Marchese et al. (17) applied the relationship of Maxwell (23) and found

$$\epsilon = 2\left(\frac{\kappa_L - \kappa_{LG}}{2\kappa_L + \kappa_{LG}}\right) \tag{12}$$

where κ_L and κ_{LG} are the measured conductivities of the liquid (pulp) and the liquid–gas mixture, respectively.

The void fraction can also be estimated from measurements of the pressure in the headspace in the downcomer. In the absence of dynamic effect, ϵ can be calculated from simple hydrostatic pressure considerations. Thus a pressure balance over the downcomer contents yields

$$P_2 - P_1 = \rho_m g h \tag{13}$$

where P_1 and P_2 are the pressures in the headspace and in the discharge end of the downcomer, respectively; h is the height of the dense foam in the downcomer; and ρ_m is the average density of the two-phase mixture inside the downcomer. When the gas density is negligible compared with the liquid density, it can be shown that ϵ is given by

$$\epsilon = 1 - \frac{\rho_m}{\rho_L} \tag{14}$$

Thus from Equation (14) we have

$$\epsilon = 1 - \frac{(P_2 - P_1)}{\rho_L g h} \tag{15}$$

Dynamic effects can be included by application of the momentum principle to the froth zone. The sum of the forces acting on the froth is equal to the gain in momentum flow rate between inlet and outlet, so

$$(P_1A_d - P_2A_d) + \rho_m g h A_d = \rho_m U_m(Q_L + Q_G) - \rho_L U_j Q_L - \rho_G U_G Q_G \quad (16)$$

where A_d is the area of cross-section of the downcomer and Q_G and Q_L are the gas and liquid flow rates, respectively. Ignoring the term in the gas density, we find:

$$\epsilon = 1 - \frac{(P_2 - P_1)}{\rho_L g h} + \frac{U_j A_j}{g h A_d}\left(U_j\left(1 - \frac{A_j}{A_d}\right) - \frac{Q_G}{A_d}\right) \quad (17)$$

where A_j is the cross-sectional area of the jet. It is seen by comparison with equation (15) that a dynamic correction term has been introduced into the expression for the void fraction. The correction is usually significant, contributing 25 to 50% of the calculated overall void fraction, depending on conditions.

H. Carrying Capacity

The carrying capacity *Ca* is the limiting or maximum concentrate production rate per unit of area of cell cross-section, usually expressed as concentrate solids rate (g/min) per unit of available cell cross-sectional area (cm^2). The carrying capacity is strongly influenced by the gas flow rate and the size of the bubbles in the froth discharging at the overflow lip, since these two factors influence the rate of surface area discharge into the launder. The mass of the hydrophobic particles that can be carried by the froth varies directly with the surface area. The other important factor is the size of the particles, because when a layer of particles is adhering to a gas–liquid interface, the mass of particles per unit of interfacial area varies directly as the mean particle size.

Carrying capacity limitations generally apply where high-grade streams are treated, as in cleaning applications, where the bubbles can easily become fully loaded with particles. The recovery is then determined by the carrying capacity rather than by the flotation kinetics.

The expected carrying capacity of conventional columns has been given by Espinosa-Gomez et al. (24) as

$$Ca = \alpha d_{80} \rho_p \quad (18)$$

where d_{80} is the size at which 80% by mass of the concentrate passes, expressed in μm, and ρ_p is the density of the particles (g/cm^3).

In conventional columns, the carrying capacity depends on column diameter. The parameter α has been found to be 0.068 in small columns (as reported by Espinosa-Gomez et al. (24) for a 50-mm column). For larger

columns, up to 1.0 m diameter, Finch and Dobby (19) give $\alpha = 0.05$; and for columns greater than 2.0 m diameter, $\alpha = 0.035$ (25).

Figure 13 shows carrying capacities measured by Atkinson et al. (21) as a function of the washwater ratio in a Jameson cell treating coarse chalcopyrite (autogenous mill discharge, $d_{80} = 400\ \mu m$). It is seen that the maximum carrying rate is strongly influenced by washwater addition.

These data show that the carrying capacity for a Jameson cell must be defined at a particular washwater ratio. For maximum concentrate grade and recovery, it is generally necessary to aim for a washwater ratio of 1.0 or just slightly lower. Thus it would be appropriate to define the carrying capacity at a washwater ratio of 1.0. In all Jameson cell applications, concentrate carrying capacities have been shown to be at least as high as the values predicted for conventional columns using Equation (18).

V. APPLICATIONS

A. General

Table 1 shows a summary of sites employing Jameson cells in mineral or coal flotation applications. In most applications, the Jameson cell is capable of providing a final grade concentrate in a single stage, providing the

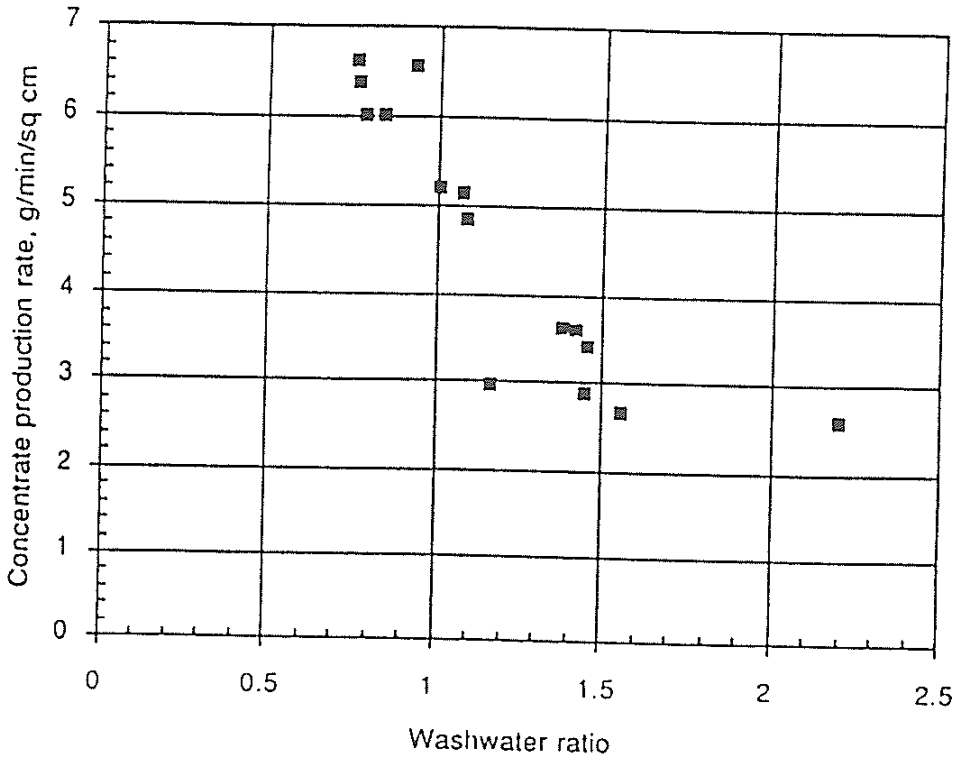

Figure 13 Concentrate production rate as function of washwater ratio for coarse chalcopyrite flotation, showing a strong reducing trend as washwater ratio is increased.

Table 1 Summary of Jameson Cell Sites (January 1993).

Company	Location	Project
Mount Isa Mines	Mount Isa, Australia	Lead/Zinc slimes
Mount Isa Mines	Mount Isa, Australia	SX-EW
Mount Isa Mines	Hilton, Australia	Low-grade middlings
Mount Isa Mines	Hilton, Australia	Lead cleaning
Peko Mines	Warrego, Australia	Copper cleaning
Amalg Syndicate	Moonta, Australia	Copper cleaning
Mamut Copper	Malaysia	Copper cleaning
Newlands Coal	Queensland, Australia	Fine coal
Amalg Syndicate	Spargoville, Australia	Nickel cleaning
Amalg Syndicate	Spargoville, Australia	Nickel roughing
Kidd Creek	Timmens, Canada	Copper/Zinc
Mount Isa Mines	Mount Isa, Australia	Fine zinc cleaning
Western Mining Corp	Olympic Dam, Australia	SX-EW
Phelps Dodge	Morenci, USA	SX-EW
Cons Murchison	South Africa	Antimony/gold
Matos Blancos	Chile	Copper cleaning
C.C.P.	Collinsville, Australia	Fine coal
Sth Atlantic Ventures	Oracle Ridge, USA	Copper roughing
White Mining	Nth Goonyella, Australia	Fine coal
BHP Australia Coal	Blackwater, Australia	Fine coal
Girilambone	NSW, Australia	SX-EW

values are sufficiently liberated and washwater is applied (where necessary). The Jameson cell is efficient for the recovery of the full range of particle sizes experienced in flotation feed streams. Examples of extremes include the recovery of coal slimes (d_{80} = 25 μm) and very fine sphalerite/galena particles (d_{80} = 10 μm) at the lower end of the particle size spectrum and, at the coarse end of the range, coal particles up to 1000 μm and chalcopyrite particles up to 400 μm.

Details of the metallurgical performance of operating Jameson cells have been given in a number of papers. Kennedy (26) described some of the early full-scale applications, in the lead/zinc concentrators at Mt. Isa, Queensland, and Hilton, Queensland; at the copper concentrator at the Peko Warrego mine, Tennant Creek, Northern Territory; and at the Newlands Coal operation in the Bowen Basin, Queensland, all in Australia.

The commissioning and operation of the Peko Warrego copper flotation cells has been described by Jameson et al. (27). The original concentrator produced a concentrate of 23% copper from a chalcopyrite ore containing pyrite, magnetite, hematite, and quartz, with traces of covellite and bis-

muthinite. The reason for the Jameson cell installation was to increase the concentrate grade from 23 to 28% or better, in order to reduce transport costs. Two 1.4-m circular cells were installed and commissioned in April 1990, taking a feed of up to 40 tph dry solids at 35% solids in the slurry. The required grade increase, obtained in the original pilot-plant tests, has been proven in plant operation.

A description of the Jameson cell installations at the Mt. Isa and Hilton mines has been given by Jameson and Manlapig (28) and Clayton et al. (29).

The flotation of fine coal slimes at the Newlands Coal operation has been described by Jameson et al. (30). The washery has an output of 1200 tph of coal, which is washed mainly in Batac jigs. The water stream from the jigs is allowed to settle and is returned for reuse. A side stream of 1250 m^3/h is taken off to prevent accumulation of slimes in the circuit, and previously this bleed stream had been sent to a tailings dam. However, the solids in the stream were in the range 3 to 8%, representing a considerable loss in ultrafine coal, around 200,000 tpa. Accordingly it was decided to recover the very fine coal, whose d_{50} is 22 μm, by flotation. Tests with mechanical cells showed that it would not be possible to recover the coal at the required ash level (12% maximum) except at unacceptably low yields, but with the Jameson cell it was found that the required ash level could readily be achieved, without the use of washwater. With a single stage of operation, the combustible recovery was 70%, and with two stages the overall recovery was 90% or better. A full-scale installation was commissioned in early 1990 and has operated ever since. Large installations are scheduled to start in 1993 at two other coal washeries in the Bowen Basin, at the BHP Australia Coal Blackwater mine and the North Goonyella joint venture.

B. Rougher Applications

The Jameson cell has been successfully employed in roughing applications and can produce a concentrate of final grade straight from run-of-mine ore. In such cases, it is possible to upgrade the capacity of a mill that has been operating with conventional flotation machines. The Jameson cell is then used as a scalper to remove a significant proportion of the feed, removing the load from the rest of the existing circuit, which can then be used to recover and clean the tails from the Jameson cell.

An interesting set of data has been obtained when a Jameson cell was set up to treat an autogenous mill discharge stream, on a chalcopyrite ore. Figure 14 shows the overall grade-recovery performance of the Jameson cell for single stage treatment of this stream. The average recovery was

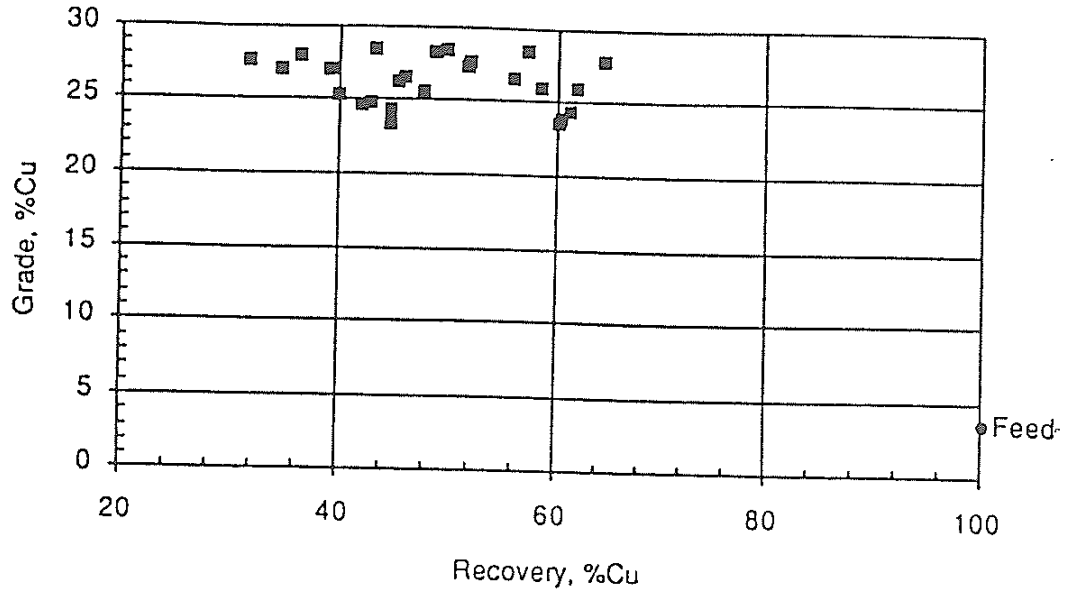

Figure 14 Grade-recovery data for single-stage Jameson cell flotation of discharge stream from autogenous mill discharge, chalcopyrite flotation circuit. Feed size d_{80} = 400 μm.

50%, at a concentrate grade of 27% Cu, from a feed grade of 3% Cu. The size analyses of the feed and the corresponding concentrate are shown in Figures 15 and 16, respectively. The d_{80} of the feed is of the order of 400 μm, while the d_{80} of the concentrate is 50 μm; most of the floatable particles are in the <20 μm fraction.

These data demonstrate the wide-ranging capability of the Jameson cell as an excellent flotation machine, capable of treating all particle sizes typically encountered in mineral processing.

VI. CONTROL REQUIREMENTS

The principal control requirements for a Jameson cell are

1. froth depth
2. washwater ratio

Froth depth control is essential for concentrate grade stability. It can be readily achieved by some type of direct or indirect level sensor (e.g., bubble pressure probe, diaphragm pressure sensor, ultrasonic sensor, float level indicator) or by a simple gravity overflow. In most applications the froth depth is between 300 and 800 mm, although for high-recovery operations where grade is not so important, froth depths as low as 50 mm are used. Where washwater is used, some measure of control is desirable in order to maximize recovery while maintaining required concentrate grade. There is

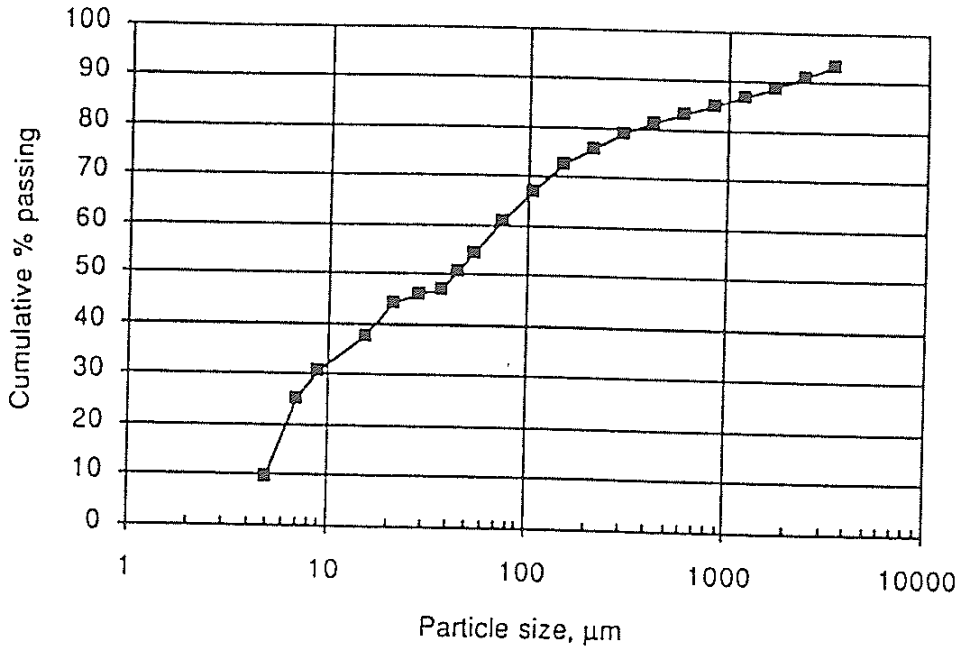

Figure 15 Cumulative size distribution of chalcopyrite flotation feed, autogenous mill discharge.

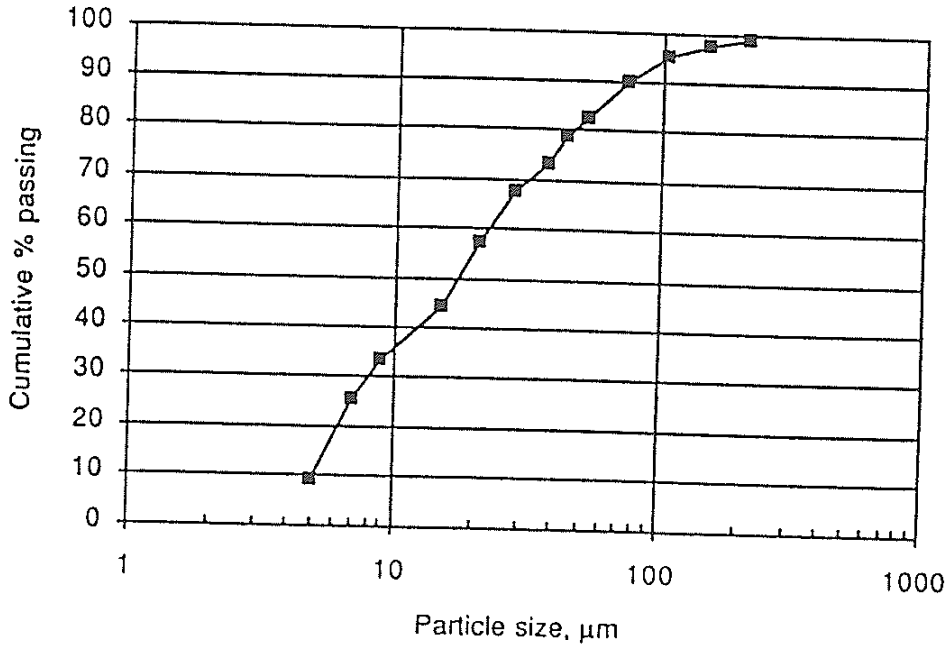

Figure 16 Cumulative size distribution, concentrate from flotation of autogenous mill discharge; $d_{80} \approx 50\ \mu m$.

some latitude in that a high grade is usually achieved for all washwater ratios greater than 1, but recovery may suffer if too much washwater is used.

Aeration of pulp occurs in the Jameson cell in the downcomer. In order to cope with feed changes, it is customary to design the cell for a maximum expected flow rate. Variations in feed can be dealt with by a number of strategies, including a variable-speed drive on the feed pump, controlling make-up water additions in the feed sump, and recycling of tails or an intermediate stream to maintain a constant flow. The cell design has been developed so that isolation of downcomers in conjunction with suitably positioned baffle plates allows fractions of the cell to be operated without affecting J_g or other design fundamentals. The solution chosen depends on the circumstances pertaining in the plant.

VII. AMENABILITY TESTING

Amenability testing is the term used to cover pilot plant testing for the purpose of assessing a technology for a given application. Table 2 provides a matrix covering the ranges of variables that should be tested in order to evaluate the capabilities of a Jameson cell fully.

In particular applications, some of the conditions may be omitted or given lower importance, e.g., mineral cleaning applications would always require washwater, whereas roughing applications or coal flotation may not. Each test should be repeated at least three times to ensure that experimental outliers are identified.

Table 2 Jameson Cell Amenability Testing Program for a Given Stream.

	Washwater ratio			Froth depth (mm)			Air/feed ratio		
Test	0	0.5	1.0	250	500	750	0.4	0.6	0.8
1	*			*				*	
2		*		*				*	
3			*	*				*	
4	*				*			*	
5		*			*			*	
6			*		*			*	
7	*					*		*	
8		*				*		*	
9			*			*		*	
10			*		*		*		
11			*		*				*

As described earlier, the washwater ratio is an extremely important variable, particularly in mineral slurry applications. For pilot-plant trials, washwater requirements can easily be estimated by collecting and weighing a timed concentrate sample. From knowledge of the approximate concentrate percent solids, the concentrate water rate can be found, which then allows setting of washwater addition to a nominated washwater ratio. In the absence of measured solids contents, it can be assumed as a good approximation that the flow rate of water in the concentrate (L/min) is the same numerically as the flow rate of froth concentrate (kg/min). The procedure should be repeated after initially setting up washwater addition, as the addition of washwater itself affects concentrate recovery rate.

ACKNOWLEDGMENTS

A worldwide exclusive license has been granted to MIM Holdings, Ltd., 400 Ann Street, Brisbane 4000, Australia, for the use and sale of the Jameson cell for metallurgical purposes. We are grateful to MIM Holdings, Ltd for their assistance in the preparation of this article. We also acknowledge the assistance of J. A. Finch, M. H. Moys, G. Harbort, and M. Marchese. One of us (BWA) acknowledges the support of an Australian Post-graduate Research Award, in conjunction with MIM Holdings, Ltd. and The University of Newcastle Research Associates Limited (TUNRA).

REFERENCES

1. G. J. Jameson, A new concept in flotation machine design, *Min. Met. Process.*, Feb., 44–47. (1988).
2. D. H. Norris, Apparatus for separating the metallic particles of ores from the rocky constituents thereof, US Patent 873586, 10 December (1907).
3. A. F. Taggart, *Handbook of Mineral Processing*, Wiley, New York, pp. 12–61. (1927).
4. G. J. Jameson, "Flotation Cell Development," Proc. Ann. Conf., Aus. Inst. Min. Metall., pp. 25–31 (1992).
5. M. J. McCarthy and N. A. Molloy, Review of stability of liquid jets and the influence of nozzle design, *Chem. Eng. J.*, *7*: 1–20. (1974).
6. M. J. McCarthy, "Entrainment by plunging jets," Ph.D. Thesis, University of Newcastle, Australia, 1972.
7. G. M. Evans and G. J. Jameson, "Prediction of the Gas Film Entrainment Rate for a Plunging Liquid Jet Reactor," AIChE Spring National Meeting, Houston, paper 34G (1991).
8. J. O. Hinze, Fundamentals of the hydrodynamic mechanism of splitting in dispersion processes, *AIChE J.*, 1: 289–295. (1955).
9. G. K. Batchelor, *Proc. Cambridge Philos. Soc.*, *41*: 359. (1951).

10. G. M. Evans, G. J. Jameson, and B. W. Atkinson, Prediction of the bubble size generated by a plunging liquid jet bubble column, *Chem. Eng. Sci.*, *47*: 3265–3272. (1992).
11. G. M. Evans, "A study of a plunging jet bubble column," Ph.D. Thesis, University of Newcastle, Australia, 1990.
12. D. T. Dumitrescu, Flow past an air-bubble in a vertical pipe, *Z. Angew. Math. Mech.*, *23*: 139–149. (1943).
13. R. Pal and J. H. Masliyah, Flow characteristics of a flotation column, *Can. Metall. Q.*, *29*(2): 97–103. (1990).
14. D. A. Langberg and G. J. Jameson, The coexistence of the froth and liquid phases in a flotation column, *Chem. Eng. Sci.*, *47*: 4345–4355. (1992).
15. M. Xu, J. A. Finch, and A. Uribe-Salas, Maximum gas and bubble surface rates in flotation columns, *Int. J. Miner. Process.*, *32*: 233–250. (1991).
16. S. E. Sanchez-Pino and M. H. Moys, "Characterisation of Co-Current Downwards Flotation Columns," Column '91, Proceedings of an International Conference on Column Flotation (G. E. Agar, B. J. Huls, and D. B. Hyma, Eds.), Sudbury, Ontario, July 1991, Vol. 1, 341–355 (1991).
17. M. M. Marchese, A. Uribe-Salas, and J. A. Finch, Measurement of gas holdup in a three-phase concurrent downflow column, *Chem. Eng. Sci.*, *47*: 3475–3482. (1992).
18. M. M. Marchese, A. Uribe-Salas, and J. A. Finch, "Hydrodynamics of a Downflow Column," to be presented at XVIII International Mineral Processing Congress, Australasian Institute of Mining and Metallurgy, Sydney, Australia, 23–28 May (1993).
19. J. A. Finch and G. S. Dobby, *Column Flotation*, Pergamon Press, Oxford. (1990).
20. J. A. Finch and G. S. Dobby, Column flotation: a selected review. Part I, *Int. J. Miner. Process.*, *33*: 343–354. (1991).
21. B. W. Atkinson, P. T. Griffin, G. J. Jameson, and R. Espinosa-Gomez, "Jameson Cell Test Work on Copper Streams in the Copper Concentrator of Mount Isa Mines Limited," to be presented at XVIII International Mineral Processing Congress, Australasian Institute of Mining and Metallurgy, Sydney, Australia, 23–28 May (1993).
22. R. Chatiar, "Report on Test Work on the Operating Parameters of the Jameson Cell," Internal Report, Department of Chemical Engineering, University of Newcastle, February (1992).
23. J. C. Maxwell, *A Treatise on Electricity and Magnetism*, 3rd ed., Vol. I, Part II, pp. 435–449, Oxford University Press, London (1892).
24. R. Espinosa-Gomez, J. A. Finch, J. B. Yianatos, and G. S. Dobby, Flotation column carrying capacity: particle size and density effects, *Miner. Eng.*, *1*(1): 77–79. (1988).
25. R. Espinosa-Gomez and N. W. Johnson, "Technical experiences with conventional columns at Mount Isa Mines Limited," Column '91, Proceedings of an International Conference on Column Flotation (G. E. Agar, B. J. Huls, and D. B. Hyma, Eds.), Sudbury, Ontario, July 1991, pp. 511–524 (1991).
26. A. Kennedy, The Jameson flotation cell, *Min. Mag.* October (1990).

27. G. J. Jameson, G. Harbort, and N. Riches, "Development and Application of the Jameson Cell," Proc. 4th Mill Operators Conference, Burnie, Tasmania, 10–14 March 1991; Melbourne: The Australasian Institute of Mining and Metallurgy (1991).
28. G. J. Jameson and E. V. Manlapig, "Applications of the Jameson Cell," Column '91, Proceedings of an International Conference on Column Flotation (G. E. Agar, B. J. Huls, and D. B. Hyma, Eds.), Sudbury, Ontario, July 1991, pp. 673–687 (1991).
29. R. Clayton, G. J. Jameson, and E. V. Manlapig, The development and application of the Jameson cell, *Miner. Eng.*, *4*(7–11): 925–933. (1991).
30. G. J. Jameson, M. Goffinet, and D. Hughes, "Operating Experiences with Jameson Cells at Newlands Coal Pty Ltd, Queensland," Proc. 5th Australian Coal Preparation Conference, Australian Coal Preparation Society, Newcastle, NSW, Australia, 12–17 May (1991).